HEFAT2012
9th International Conference on Heat Transfer, Fluid Mechanics and Thermodynamics
16 – 18 July 2012
Malta

SIMULATION OF MICRO-SCALE IONIZED GAS SYSTEMS FOR AEROSPACE APPLICATIONS

Manish Jugroot
Department of Mechanical and Aerospace Engineering
Royal Military College of Canada
Kingston, Ontario, K7K 7B4
Canada
E-mail: jugroot-m@rmc.ca

ABSTRACT

Small scale ionized gases are interesting for a number of high-technology aerospace applications, such as active flow control and spacecraft electric propulsion. Due to the inherent difficulty to perform experiments at this scale (space and time), modeling and simulation appear as a powerful complementary tool to investigate the underlying phenomena. A numerical model is described for simulation of gas and plasma dynamics in micro-scale gaps. The two-dimensional time-dependant model is described and applied with emphasis on terms involving coupling among the fluid, the plasma and applied electric/magnetic fields. The populations are studied from an initial cloud and transients are observed to be particularly important. The governing factors in flow actuation or propulsion are discussed in terms of the spatial and temporal evolution of the plasma and fluid dynamics. Hence, gas heating, electrohydrodynamic effects and body forces are compared to assess the importance of each effect, highlighting the close interaction between the fluid and ionized gas in microplasmas.

INTRODUCTION

Micro-scale plasmas or microplasmas are very interesting for miniaturization of devices for aerospace applications such as electric spacecraft propulsion and plasma-based flow control [1-2]. Due to the localized control and interaction of the charged species with the gas and electric/magnetic fields, microplasmas can potentially enhance or modify the exhaust velocity in electric thrusters and flow control devices. Microplasmas have unique features and more modeling and plasma diagnostics are needed to identify phenomena specific to microdischarges [3]. The microplasma investigated is of a generic form in order to understand and compare competing effects of paramount importance, namely surface and volume effects. There are numerous unresolved questions to elucidate in order to better understand the phenomena involved in microplasmas where complex behaviors are observed (for example fluid heating). For instance, concerning the surface effect responsible for the maintain of the discharge, secondary emission at the cathode appears as a very important parameter [4]. As a matter of fact, the critical nature of secondary emission is evident in microplasmas deviations, from usual characterizing laws such as Paschen’s law, are observed [5]. On the other hand, volume effects such as ionization are also of high importance due to the high gradients involved in short distances and localized effects. Furthermore, in small-space discharges, the energy transfer to the neutral gas as a result of collisions between charged and neutral particles, induces energy gradients and can in turn induce a convective movement of neutral particles [6-7].

In the present study, both surface and volume effects are investigated. To comprehend the complex nature of volume effects, several phenomena responsible for ionization are considered and discussed. The effect of an applied magnetic field is also included in order to capture the superimposed effect on plasma populations. Moreover, gas heating and fluid dynamics are also important considerations – the formalism described therefore puts forward a global approach (fluid and plasma dynamics) for a self-consistent numerical modeling of microplasmas.

GOVERNING EQUATIONS AND NUMERICAL METHOD

The self-consistent formalism coupling all the different species is described in the summary provided in this section. The neutral dynamics is governed by the macroscopic hydrodynamic equations of a compressible and viscous fluid comprising conservation equations of densities of mass $m_N N$, momentum $m_N N\, v_N$ and total energy ε respectively:

$$\frac{\partial m_N N}{\partial t} + \nabla[m_N N\ v_N] = 0\,, \tag{1}$$

$$\frac{\partial m_N N\ v_N}{\partial t} + \nabla[m_N N\ v_N v_N] =$$

$$n_s \frac{m_N m_s}{(m_N + m_s)} \upsilon_{sN}(v_s - v_N) - \nabla pI - \nabla \tau \tag{2}$$

$$\frac{\partial \varepsilon}{\partial t} + \nabla[\varepsilon\ v_N] = \nabla Q - \nabla[v_N.(pI + \tau)] + f_t J.E \tag{3}$$

$m_N, N\ , v_N, p$ and *T* are the mass, density, velocity, pressure and temperature of the gas respectively. υ_{sN} is the collision frequency between charged and neutral particles, ε is the total energy, the heat flux is Q and the viscous tensor τ .

The three equations describing the neutral dynamics are not only strongly coupled but are moreover dependent on the charged particles dynamics via the terms $n_s \frac{m_N m_s}{(m_N + m_s)} \upsilon_{sN}(v_s - v_N)$ and $f_t J.E$. Indeed, these terms represent respectively the action of the plasma on the neutral gas by two modes of transfer namely momentum (due to convection) and energy transfer (due to Joule heating). This implies that the neutral dynamics is conditioned by the charged particle dynamics which can be represented by the conservation equations for charged particles.

Equation 4 shows the conservation equation for plasma charged species (*s*: electrons and ions respectively, for the plus and minus signs in second RHS term). For ions, the momentum equation [8] was also solved in order to account for the magnetic field terms in our simulations. Equation 5 depicts the Poisson equation describing the electric field *E*, including space charge:

$$\frac{\partial n_s}{\partial t} + \nabla\{\pm n_s \mu_s N \frac{E}{N} - D_s \nabla[n_s] \pm \frac{n_s \mu_s}{c}[v_s B]\} = S_s \tag{4}$$

$$\Delta V = -\frac{e(n_i - n_e)}{\varepsilon_0}; \quad E = -\nabla V \tag{5}$$

The subscript *s* refers to the particle considered, n_s is the density (n_e and n_i are electron and positive ion densities), v_s the mean velocity, S_s the source term, D_s the diffusion coefficient, μ_s the mobility and *e* the electron charge.

The discharge is initiated by releasing an electron swarm near the cathode and the evolution is followed till the stage of particle over-amplification. The magnetic field is applied in the perpendicular direction. The discharge is maintained by secondary emission and amplified by ionization processes (direct, stepwise and Penning ionizations are considered). Under these conditions, the source term of Eq. (4) can be written as:

$$S_e = S_i = v_{ion} n_e + k_{em} n_e n_m + k_{pm} n_m n_p\,. \tag{6}$$

The first right hand side term represents direct ionization, the second term stepwise ionization, and the third is due to Penning ionization. k_{pm} is a rate coefficient, n_p the density of impurities and n_m the metastables. Secondary emission (γ) has been shown to be a critical parameter in microplasmas and two values are discussed in the present paper.

The conservation equations are solved by the flux corrected transport (FCT) algorithm [9] with time-splitting. The electric field is solved by Fast Fourier Transform (FFT) following both *x* and *y* directions.

RESULTS AND DISCUSSION

The competing effects of surface and volume phenomena are discussed in microplasmas. A Helium microcavity (200 μm) at atmospheric pressure and at 293 K with an applied DC voltage of 240 V is the base case of the investigation. The effect of a magnetic field [10-11] is considered and its subsequent influence on the plasma and neutral gas dynamics is measured. Different values of secondary emission are also investigated and their impact on both the localized and general behavior on fluid and charged species dynamics are discussed.

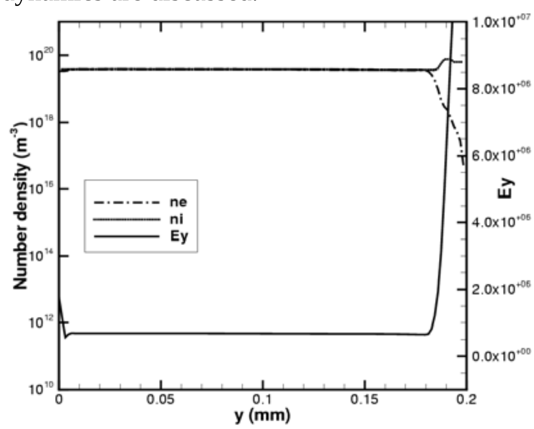

Figure 1 Electron and ion density and longitudinal electric field (Helium; t=96 ns; V=240 V; B=0.3 T; γ= 0.1; Anode y=0 mm and Cathode y= 0.2 mm).

The fundamental phenomenon is common (for the first instants of the plasma amplification) to all cases and is summarized as follows. The primary electron swarm is exposed to a strong convective effect and begins to move towards the anode, which is reached after a few nanoseconds, while the ions are slowly attracted towards the cathode. The primary electrons are thus rapidly absorbed and the discharge is thereby sustained by the secondary emission at the cathode. For all cases (of secondary emission investigated or electric and magnetic field applied) the trends are qualitatively similar as discussed hereafter. The density profiles do not change significantly during the first amplification phase during which spatial gradients are conserved, implying more uniform discharge characteristics (exponential longitudinal growth, nearly constant temporal growth rate and transverse population profiles close to Gaussian shape). During the first period, the ion space charge gradually builds up as a consequence of the relatively small ion mobility compared to the electronic mobility. The corresponding electric field is equal to the applied electric field at that point.

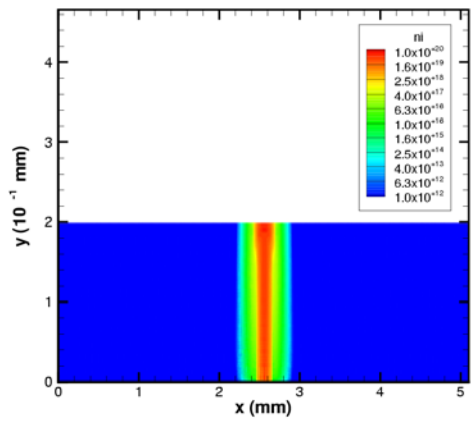

Figure 2 Ion density (m^{-3}) showing structure of discharge (Helium; t=96 ns; V=240 V; B=0.3 T; γ= 0.1; Anode y=0 mm and Cathode y= 0.2 mm).

The next sequence is governed by the strong electric field induced by the space charge. As a matter of fact, the electric field increases due to the excess of ionic species compared to electronic ones. The onset of space charge is measured and its effects can be clearly seen for example at 95 ns, a later stage in the evolution (Figure 1). The differences in ion and electron densities lead to a strong local electric field which is conserved and builds up continuously as the net charge increases. This accumulation in turn enhances ionization processes, and thereby increases the ion density as electrons are rapidly evacuated to the anode due to the strength of the electric field. Consequently, the electric field is further increased, thus reinforcing the whole process. The electric field profile allows an increasing number of electrons to be generated by secondary emission, but is overall insufficient to compensate for the lack of electrons in the cathode fall region.

For this phase and subsequent evolution of the gas/plasma system, the evolution is different based on the complex interrelated between surface and volume effects highlighted in the microplasma.

The application of a magnetic field changes the particle amplification in a clearly observable fashion. The first and second amplification phases are the same. However, a constriction in the plasma population is observed close to the cathode as depicted in Figure 2 for ion densities. This is due to the magnetic field contributing to the amplification and accumulation of particles. The electric field is relatively low in that localized region leading to a competition between drift and amplification. The drift being comparatively low leads to a radial accumulation. The enhanced constricted behavior has also been qualitatively observed in a low pressure case [8].

The amplification can in turn lead to a rise in temperature of the neutral gas and pressure. The initiation of depletion or rarefaction (N decreasing) is also observed. Interestingly, the reduced electric field could play an increasingly important role in the subsequent plasma evolution. The ionization terms are calculated for the presence of a magnetic field superimposed to the electric field. It can be seen that direct ionization term as described in equation 6 is several orders of magnitude higher as seen in Figure 3. It is also important to note that the influence of Penning ionization is also enhanced in Helium.

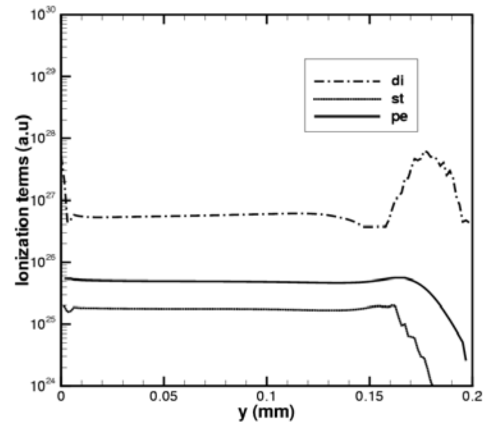

Figure 3 Ionization terms: Direct, Stepwise and Penning (Helium; t=96 ns; V=240 V; B=0.3 T; γ= 0.05; Anode y=0 mm and Cathode y= 0.2 mm).

The influence of surface effects due to the presence of a dielectric has already been discussed previously [4]. As a matter of fact, several modes could co-exist such as field emission. In the present case, the secondary emission which could potentially be fluctuating due to the inherent specificities of microplasmas [5] is investigated. The surface effect term encompassed by the secondary emission γ is varied between values of 0.1 and 0.05 to explore this effect.

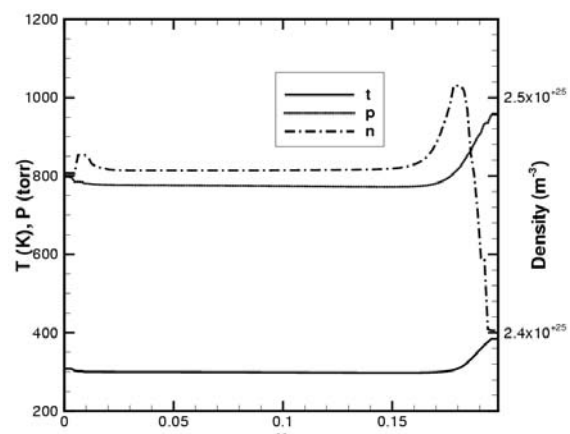

Figure 4 Distribution of gas pressure, temperature and density along the discharge axis. (Helium; t=96 ns; V=240 V; B=0.3 T; γ= 0.05; Anode y=0 mm and Cathode y= 0.2 mm).

Figure 4 shows a lower value of secondary emission and the evolution of the plasma. Heating and depletion of the gas is observed at 134 ns for an applied magnetic field and a lower secondary emission. The gas heating peaks near the cathode where the neutral gas rises to 400 K. An initiation of rarefaction of the neutral gas is also observed. The accumulation of energy and momentum effects creates a high pressure zone of 950 torr near the cathode. This energy and momentum accumulation triggers the movement of the neutral gas and induces a neutral depopulation.

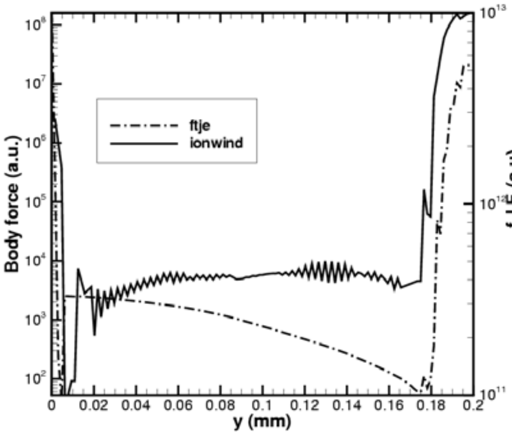

Figure 5 Distribution of terms, body force and Joule heating, along the discharge axis. (Helium; t=134 ns; V=240 V; B=0.3 T; γ= 0.05; Anode y=0 mm and Cathode y= 0.2 mm).

The Joule heating term $f_t J.E$ is also known to play a very important role in plasma-based actuators [12] and plasma-enhanced electric spacecraft propulsion. In the global physical phenomenon, the Joule energy term is competing with the body force (force per unit volume) term $F_B = e(n_i - n_e)E$. In fact, the former could actually be the leading term in certain electrode and flow configurations [12]. Figure 5 show the two terms in arbitrary units in order to understand the profiles and trends. Interestingly, the ion wind related term is significantly higher once the gas heating cause by Joule heating is initiated. The latter is an energy-related effect whereas the latter is a momentum-based effect. The difference in charged particle species and the space charge expressed by the inhomogeneous electric field confirms that both effects are larger in the cathide region. Furthermore, in the case of pulsed discharges [13] of interest for these applications, memory effects of the plasma or neutral gas effect could be embedded in the subsequent pulses, as the previous event could live over the afterglow period as the frequency of the recurrent discharges is very high. The constriction of the plasma canal can also have an enhancing contribution to the amplification of charges.

CONCLUDING REMARKS

The charged particle distribution and amplification observed in this general microplasma geometry study are to a great extent specific to small gaps as the electrons drift very rapidly across and are readily absorbed. We have shown several phases in the evolution of helium microplasmas initiated by an electronic swarm and maintained by secondary emission and ionization: surface and volume effects. The fluid-plasma self-consistent formalism implemented in the present model clearly shows the prime importance of coupled effects in microplasmas. The cumulative effect of the plasma and the gas are demonstrated to be of high importance in the microplasma. In aerospace applications both components are of paramount significance, for instance in the boundary layer flow of the gas close to the actuator – and in the heating of the gas further from the surfaces, within the volume. This double combined effect if optimized could be extremely effective to modify the flow structure.

In summary, surface and volume effects are shown to be closely related and essential in microplasmas as demonstrated by self-consistent modeling. This interdependence is clearly highlighted by space charge effects and neutral heating leading to the initiation of gas depletion. The differences between different secondary emission coefficients for electrodes and the application of electric/magnetic fields have been discussed. The distribution of the species of the plasma is different but the same global features are observed. In all cases investigated, both charged and neutral effects characterize and govern the evolution of the microplasmas of high interest to electric micropropulsion devices and active flow control. Future work will also investigate open surfaces with flow as opposed to occluded gaps and will compare the results to experimental data.

ACKNOWLEDGEMENTS

The support of the Natural Sciences and Engineering Research Council of Canada (NSERC), the Technology Investment Fund (TIF/DRDC) and the Academic Research Program (ARP/RMC) are gratefully acknowledged.

REFERENCES

[1] I.D. Boyd, *Progress in Aerospace Sciences* **41**, (2005)

[2] K.H. Becker, J.G. Eden and K.H. Schoenbach, *J. Phys. D: Appl. Phys.* **38**, (2005)

[3] E. Moreau, *J. Phys. D: Appl. Phys.* **40**, (2007)

[4] M. Jugroot, P. Bayle, M. Yousfi and O. Eichwald, *J. Phys. D: Appl. Phys.* **32**, (1999)

[5] M. Klas, S. Matejcik, B. Radjenovic, M. Radmilovic-Radjenovic, *Phys. Lett. A* **376**, (2012)

[6] M. Kushner, *J. Phys. D: Appl. Phys.* **38**, (2005)

[7] M. Jugroot, *Plasma Process. Polym.* **6**, (2009)

[8] S. Surzhikov, J. Shang, *J. Comput. Phys.* **199**, (2004)

[9] J.P. Boris and D.L. Book, *J. Comput. Phys.* **135**, (1997)

[10] C. Wilson, Y. Gianchandani, *IEEE Trans. Plasma Sci.* **32**, (2004)

[12] H. Yoshiki, *Appl. Phys. Lett*. **95**, (2009)

[13] F. Iza, J. Walsh, M. Kong, *IEEE Trans. Plasma Sci.* **37**, (2009)